Materials Science & Engineering A 787 (2020) 139551

Contents lists available at ScienceDirect

Materials Science & Engineering A

journal homepage: http://www.elsevier.com/locate/msea

Short communication

Room temperature yielding phenomenon in extruded or/and aged Mg-14Gd-2Ag-0.5Zr alloy with fine-grained microstructure

R.G. Li [a], D.Y. Zhao [a], J.H. Zhang [b,*], H.R. Li [a], Y.Q. Dai [a], D.Q. Fang [c,**]

[a] School of Mechanical and Power Engineering, Shenyang University of Chemical Technology, Shenyang, 110142, China
[b] Key Laboratory of Superlight Material and Surface Technology, Ministry of Education, College of Material Science and Chemical Engineering, Harbin Engineering University, Harbin, 150001, China
[c] State Key Laboratory for Mechanical Behavior of Materials, Xi'an Jiaotong University, Xi'an, 710049, China

ARTICLE INFO

Keywords:
Magnesium alloy
Extrusion
Fine-grained structure
Yielding
Dislocation

ABSTRACT

A new phenomenon of tensile yielding plateau in the fine-grained age-type Mg-14Gd-2Ag-0.5Zr alloy is reported, which is closely related to the activation of mobile pinned-dislocations. The yielding plateau contributes ~6% strain in the peak-aged sample, while it contributes only ~2% strain in the extruded sample.

1. Introduction

Paying attention to the specific phenomenon of stress and strain after loading can help to deeply understand the deformation as well as strengthening mechanism of magnesium (Mg) alloys. The yielding phenomenon containing a yield plateau has been widely reported in steel and aluminum alloys [1–4]; however, only very few reports are referred to the yielding phenomenon in Mg alloys. Though the formation conditions and possible mechanisms for this phenomenon in Mg alloys are different in the previous reports, there Mg alloys seem to exhibit an excellent ductility when a yielding phenomenon appears during deformation at room temperature (RT) [5–10]. The extruded Mg-2.5Y (at.%) alloy with an average grain size of ~1 μm exhibits a true strain of 13.5% under tensile test and 17.0% for compressive test at RT, and the yielding phenomenon occurs in both tensile and compressive tests. The authors suggest that the yielding phenomenon may be closely related to the pinning role of solute Y atoms at the basal and prismatic <a> dislocations [5]. The obvious yielding point is also observed during the tensile process of fine-grained AZ31 alloy with an elongation of ~42% at RT, which is considered to be related to the cross-slipping of <a> dislocations and the <c+a> dislocations [6]. A similar yielding phenomenon also appears in the tensile curve of fine-grained Mg-3Gd alloy with an elongation of more than 30% [7], where the yielding point is considered to be due to lack of dislocations in initial fine-grained alloy, and activation simultaneously of numerous basal slips and non basal slips during tensile test. Extensive twinning can produce the obvious yielding plateau in the compressive stress strain curve when as-extruded coarse-grained AZ31 alloy is tested at RT, which is corresponding to the deformation course from activation of twinning to exhaustion of the twinning capacity [8]. The yielding plateau is induced in the extruded Mg-4.5Zn (wt.%) alloy with an average grain size of ~20 μm and extruded Mg–2Zn-0.5Mn (wt.%) alloy with an average grain size of ~17 μm by cooperative twinning in neighbouring grains at the onset of plasticity during compressive test along the extruded direction [9,10]. It should be noted that the vast majority of Mg alloys still have no yielding phenomenon despite the above mentioned cases.

Though the yielding phenomenon has been mentioned in the coarse-grained Mg alloys (AZ31, Mg-4.5Zn and Mg–2Zn-0.5Mn) and the fine-grained Mg alloys (Mg-2.5Y, Mg-3Gd and AZ31) [5–10], the deformation mechanism of yield plateau in different microstructure and the contribution of the yield plateau to Mg plasticity are still not fully understood, and the yielding phenomenon is rarely reported and analyzed in the fine-grained age-type Mg alloys. Recently, the high-performance age-type Mg–Gd/Mg-Gd-Ag series alloy has attracted attention [11–20]. The rare earth (RE) elements can enhance the critical resolved shear stresses (CRSS) value of basal <a> slip, but have relatively little influence on CRSS of non basal slip, which causes the more non-basal slip to contribute to deformed plasticity of Mg [21–26]. In our present

* Corresponding author.
** Corresponding author.
E-mail addresses: jinghuaizhang@gmail.com (J.H. Zhang), fangdaqing@xjtu.edu.cn (D.Q. Fang).

https://doi.org/10.1016/j.msea.2020.139551
Received 4 March 2020; Received in revised form 19 April 2020; Accepted 9 May 2020
Available online 11 May 2020

work, a high-plastic and high-strength Mg-14Gd-2Ag-0.5Zr alloy is prepared, and specially the yielding phenomenon is found in tensile test at RT. In this paper, the yielding phenomenon is analyzed as the focus, and the influence factors and mechanism are discussed. The results are helpful to design and control the microstructure of the age-type Mg alloys, and contribute to understand the deformation as well as strengthening mechanism of age-type Mg alloys with fine-grained microstructure.

2. Experimental details

The Mg-14Gd-2Ag-0.5Zr (wt.%) alloy, having the actual composition of 83.4723Mg-14.2503Gd-1.7844Ag-0.4930Zr (wt.%) detected by the X-ray fluorescence spectrometer, was prepared using the semi-continuous casting method. Purity (99.9%) Mg, Gd, Ag and Mg–33Zr (wt.%) master alloy were melted in an electronic furnace at 750 °C, and the melt was poured into the cooling crystallizer at 720 °C to prepare the billet. The cylindrical-shaped samples with height of 100 mm and diameter of 85 mm were cut from the billet. The cylindrical samples were homogenized at 505 °C for 24 h, and then quenched into warm water of above 80 °C. These homogenized samples were kept in furnace for 1 h at 400 °C, and then extruded into bars with a diameter of 16 mm at 400 °C with a cylindrical extrusion chamber temperature of 400 °C, a mold temperature of 330 °C, an extrusion ratio of 28, a low ram speed of 0.4 mm/min and subsequently quickly quenched into cold water. Some extrusion samples were aged at 200 °C.

The tensile bars with a size of 25 mm in gauge length and 4 mm in diameter were tested using a Shimadzu Autograph AG-I (500 kN) equiped with extensometer with an initial strain rate of 10^{-3}/s at RT. The tensile direction is parallel to extruded direction (ED), and 5 samples were tensile-tested under the same test parameter for test accuracy. The hardness was performed by a MH-5L Vickers hardness tester at the load of 1 kg and holding time of 15 s. The 10 indents were made in each sample to get the average value. The microstructure was characterized by a FEI Nova 400 scanning electron microscope (SEM) equipped with Oxford HKL Channel 5 electron backscattered diffraction (EBSD) detector and a Zeiss Libra 20FE transmission electron microscope (TEM) as well as a Rigaku X-ray diffractometer (XRD). The thin foil samples for TEM observation were prepared using low energy ion beam thinning technique.

3. Results

Fig. 1(a) shows the optical micrograph of the extruded Mg-14Gd-2Ag-0.5Zr sample, and it reveals the uniform microstructure with fine equiaxed dynamic recrystallized (DRXed) grains and intermetallic particles. The SEM images in Fig. 1(b) and (c) further exhibit that the average grain size is about 2 μm, and large particles are ~1.5 μm in size, while numerous fine particles are ~200 nm in size. In general, the large particles, pointed by green arrows in Fig. 1(b), are considered to be formed during the heating at 400 °C for 1 h, and continue to grow during extrusion, and the fine particles mainly distributed along DRXed grain boundaries are formed by dynamic precipitation during extrusion [12,13,20,27]. By comparing XRD results (Fig. 1d) of the solid solution-treated alloy and the extruded alloy, it can be found that the Mg_5Gd phase is formed in the extruded alloy, which should correspond to the large and fine particles found in the SEM images [12,13,20,27].

Fig. 2 shows TEM images of the extruded sample, revealing the detailed structure of DRXed grains. The dynamic precipitates with a size of ~200 nm have polygonal morphology and are mainly dispersed on the DRXed grain boundaries (Fig. 2a). The fine equiaxed DRXed grain surrounded by precipitates suggests that the grain boundary migration can be impeded by a large amount of dynamic precipitation during the extrusion with a very low extrusion rate. The DRXed grain attached to the relatively large particle (pointed by the green arrows in Fig. 2b and c) is observed, suggesting the particle stimulated nucleation effect. More importantly, the residual dislocation can be observed in the DRXed grain as shown in Fig. 2(b)–(d). In particular, the dislocation-rearranged structure (pointed by the red arrows) formed due to dislocation recovery are pinned by the granular particles (pointed by the yellow arrows). The granular particles in the DRXed grain are dynamically formed at the grain boundary of the initially nucleated DRX grain and remain in the interior of the DRX grain during the grain boundary migration caused by the grain growth. The dislocations pointed by blue arrows in Fig. 2(c)

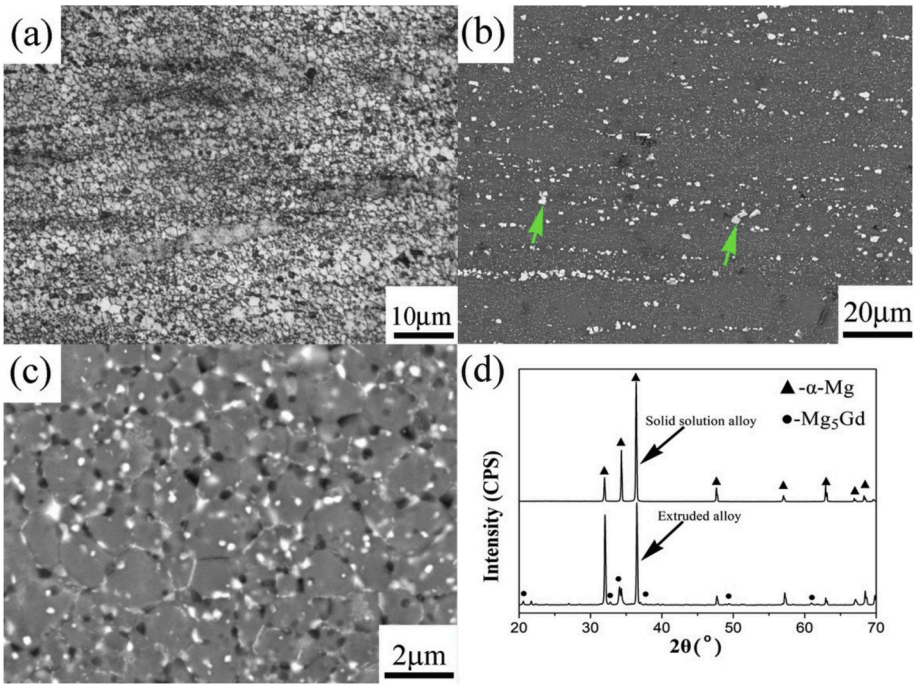

Fig. 1. Optical micrograph (a), scanning electron microscopy (SEM) image (b) and (c) of extruded Mg-14Gd-2Ag-0.5Zr sample along the longitudinal section, and X-ray diffraction pattern of the solid solution sample and the extruded sample of Mg-14Gd-2Ag-0.5Zr alloy (d).

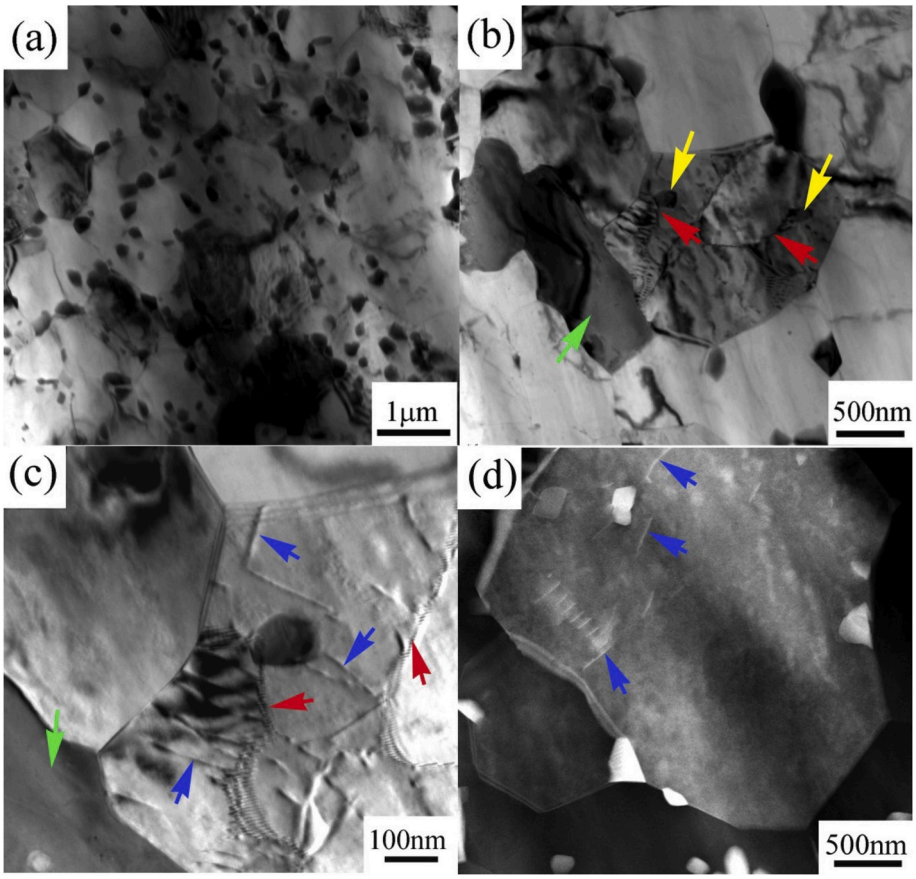

Fig. 2. Transmission electron microscopy (TEM) of the extruded Mg-14Gd-2Ag-0.5Zr sample, (a) microstructure containing the fine grains surrounded by the dynamical precipitates, (b) microstructure containing the bulk compound and the dislocation-rearranged structure near the fine DRX grain, (c) microstructure containing subgrain and dislocation, and (d) element segregation in DRX grain observed using HAADF-STEM with a electron beam parallel to Ref. [11–20]$_{Mg}$.

are restrained by the grain boundary and the dislocation-rearranged structure. This dislocation can be readily activated to be mobile dislocation when the stress is loaded, while the dislocation-rearranged structure is difficult to start due to the strain field produced by the interaction of many dislocations. The brighter contrast at the dislocation site in the DRXed grain may be contributed by the segregation of Gd/Ag (Fig. 2d), suggesting that segregation of Gd/Ag at the dislocation site may occur simultaneously with the dynamic precipitation along DRXed grain boundaries during the extrusion. It is clearly confirmed solute clustering in the interior of grains and segregation at grain boundaries in extruded Mg–Gd alloys using the HADDF-STEM observation [28].

Fig. 3 exhibits the EBSD analysis of the extruded sample. The complete dynamic recrystallization (DRX) results in a weak texture, and the maximum of intensity is only 2.68 (Fig. 3a and b). It is confirmed that some low angle boundaries exist in the DRXed grains formed during extrusion (Fig. 3c and d), which is consistent with existence of the dislocation-rearranged structure (pointed by red arrows in Fig. 2b and c). Fig. 3(e)–(f) show the Schmid factor distribution maps for the different slip systems. The average Schmid factors calculated for the basal {0001}<11–20>, prismatic {10-10}<1–210>, pyramidal {11–22}<-1-123> slip systems are 0.295, 0.32, 0.40, respectively. In Mg-RE alloys, activation of non-basal dislocation can be caused by reducing the CRSS difference between the basal slip and the non-basal slip due to the RE addition [21], and high Schmid factor for non-basal dislocations slip system facilitates the activation of non-basal dislocation, which produces a good plasticity in Mg alloys. It has been reported that the pyramidal <c+a> dislocation in the fine-grained Mg-2.5Y alloy cannot be activated due to the high CRSS during tensile deformation at RT [5], even though the higher Schmid factor of pyramidal <c+a> slip is obtained. Therefore, for the present fine-grained Mg-Gd-Ag alloy, it seems that the basal and prismatic <a> dislocation slips are possibly main deformation mode on the initial stage of plasticity during test at RT. However, it also deserves to future research whether the residual <c+a> dislocation, which is formed during hot extrusion and remains in the fine DRXed grains surrounded by the sub-micro particles, can be activated or not.

Fig. 4(a) shows the aging hardening curve of the extruded samples at 200 °C. The peak value is obtained when the aged time is 30 h (here named as peak-aged sample). Fig. 4(b) presents the typical engineering tensile curves of the extruded and peak-aged alloys tested at RT. It can be seen that the extruded alloy has high elongation and moderate strength, while the strength increases significantly but the plasticity remains unchanged after aging treatment, so that the peak-aged alloy gains both high plasticity and high strength. In particular, the obvious yielding point and the yielding plateau can be observed in the tensile curves for both the extruded and the peak-aged samples (Fig. 4c and d), and the yielding plateau contributes ~6% strain in the peak-aged sample, while it contributes only ~2% strain in the extruded sample.

Fig. 5 presents TEM images of the peak-aged sample. The dislocation-rearranged structure, pointed by red arrows in Fig.5(a), is still observed in the peak-aged sample, meaning the dislocation-rearranged structure is maybe stable when it is hold 30 h at 200 °C. It is thought that the further Gd/Ag segregation at the site of dislocation is main reason for enhancing the hardness of sample during aging. A new microstructure with the dislocation ring structure pinned by fine particles (named as pinned dislocation-ring), pointed by blue arrows shown in Fig. 5(b), can be observed in the present peak-aged Mg-14Gd-2Ag-0.5Zr alloy, which is different from β′ or γ″ precipitation reported in the previous literature

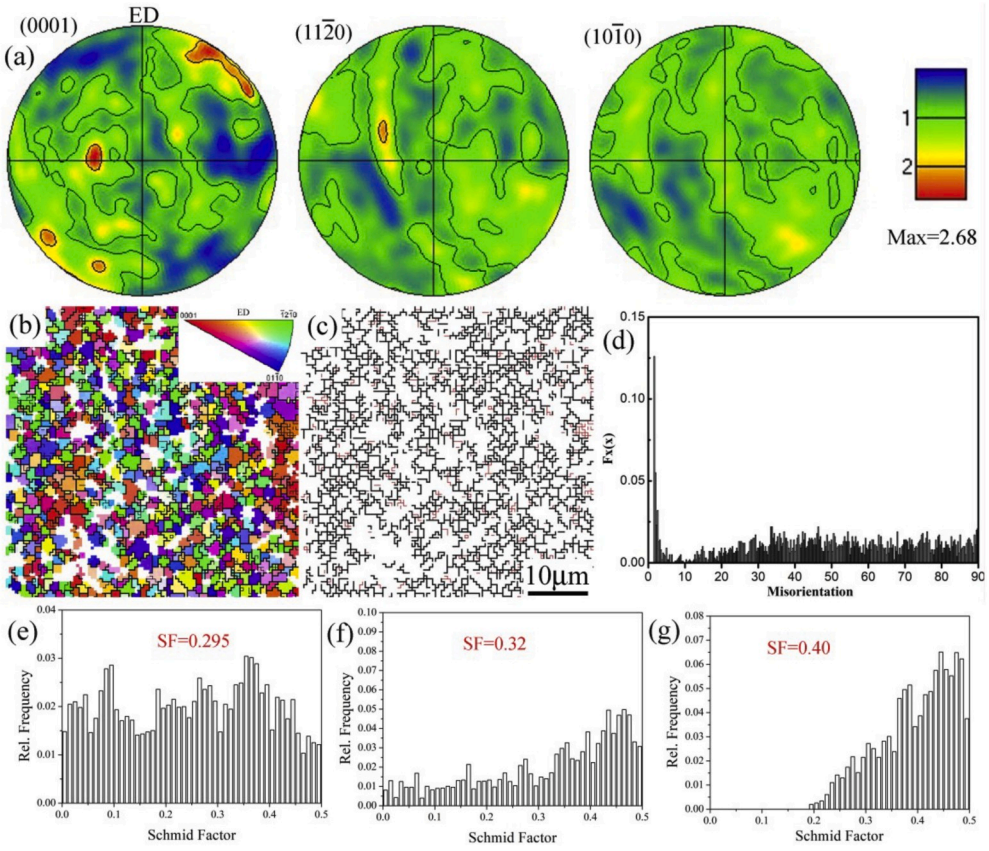

Fig. 3. Electron backscattered diffraction (EBSD) images of the extruded Mg-14Gd-2Ag-0.5Zr sample, (0002), (11–20) and (10–10) pole figure (a), inverse pole figure (IPF) maps with the reference of extrusion direction (ED) (b), the grain boundary map (c), misorientation angle distribution map (d), Schmid factor distribution maps for the {0001}<11–20> (e), {10-10}<1–210> (f), {11–22}<-1-123> (g) slip systems derived from EBSD of the as-extruded sample when it is tensile tested along the ED. The vertical direction is parallel to ED in (b) and (c). The black line and the red line in (c) represent the boundaries with misorientation angle above 15° and the boundaries with misorientation angle between 1° and 15°, respectively. (For interpretation of the references to colour in this figure legend, the reader is referred to the Web version of this article.)

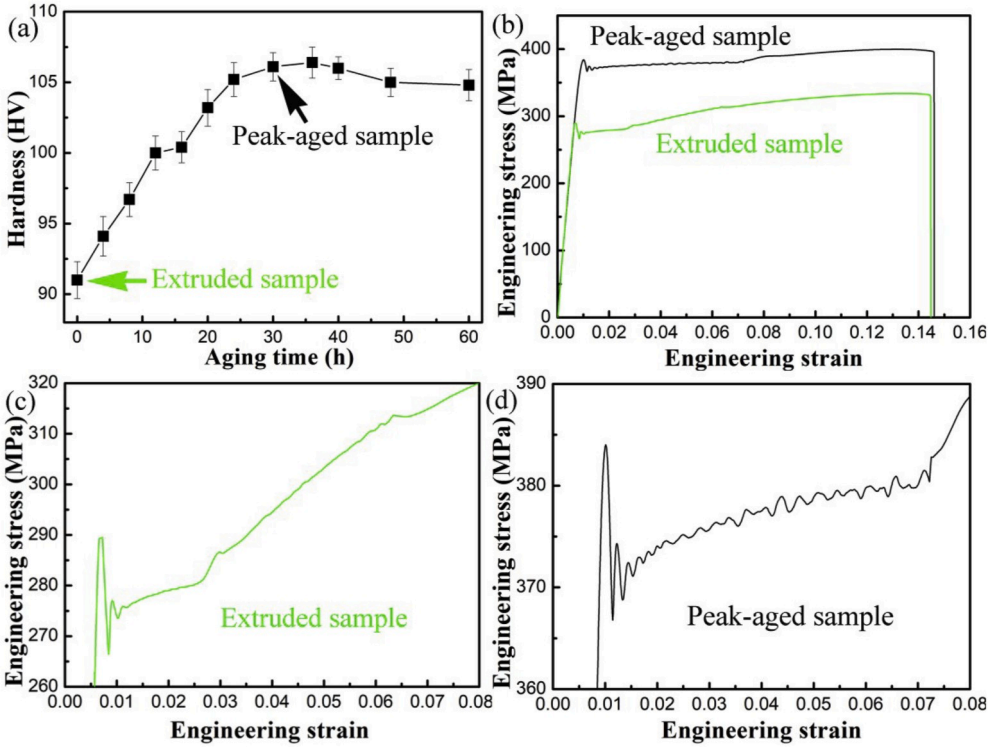

Fig. 4. (a) Aging curve of the extruded Mg-14Gd-2Ag-0.5Zr sample with a aging temperature of 200 °C, (b) engineering stress-strain tensile curve for the extruded sample and the peak-aged sample, (c) enlarging image of the yield site of the tensile curve for the extruded sample, (d) enlarging image of the yield site of the tensile curve for the peak-aged sample.Tensile direction in all test samples is parallel to ED.

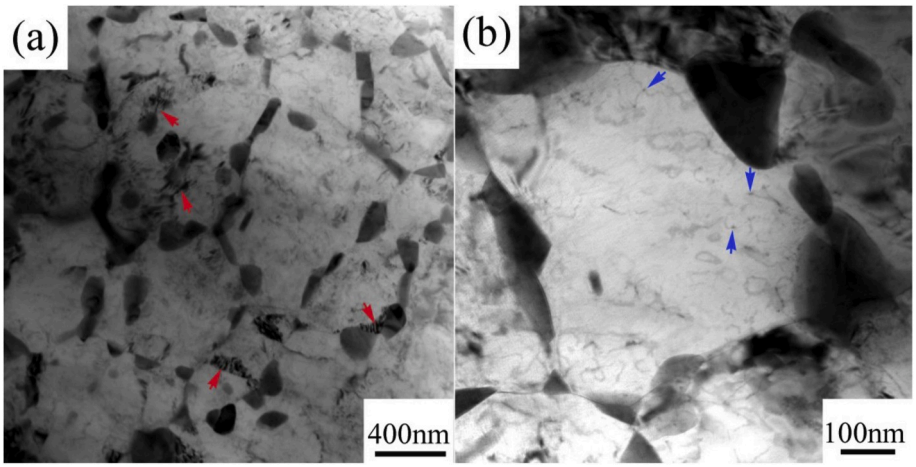

Fig. 5. TEM images of the peak-aged Mg-14Gd-2Ag-0.5Zr sample, (a) microstructure containing the dynamical precipitate and the dislocation-rearranged structure near grain boundary, (b) microstructure containing the ring-pinned structure in the interior of grains.

[13–18]. It has been reported that common precipitation processes of β′ and γ′′ phases can be suppressed by the solute segregation or new phase nucleation at the site of dislocation in the aged Mg-8.2Gd-3.8Y-1.0Zn-0.4Zr alloy processed by high pressure torsion [29,30], and the new phase nucleation at the site of dislocation has been also observed in the Mg-Gd-Ca alloy during creep [31]. The pinned dislocation-ring is maybe formed from the dissociation of dislocation-rearranged structure, and the clear formation mechanism needs further research in the future. The further segregation of solute atoms occurs accompanied by the dissociation of dislocation-rearranged structure during aging, and finally the fine precipitates can be formed at the site of dislocations (pointed by the blue arrows in Fig. 5b).

4. Discussion

4.1. Formation of the fine-grained microstructure

In this work, we consider that the formation of fine-grained microstructure in the Mg-14Gd-2Ag-0.5Zr alloy during extrusion is at least related to the following microscopic factors. The relatively large particles originated from the pre-heating stage can help DRX nucleation and impede the growth of DRXed grains. More importantly, the numerous dynamic precipitates formed along grain boundaries of DRXed grains would effectively hinder the migration of grain boundaries during the extrusion. In addition, it is easy to deduce that the diffusion speed of grain boundary is also reduced due to the decrease of grain boundary energy via the segregation of Gd and Ag atoms into the boundary of DRXed grains, which facilitates the fine-grained microstructure.

The formation of internal microstructure of fine DRXed grains can be considered from the influence of extrusion process and alloying element. In the present work, the low extrusion rate gives the sufficient time to complete the courses of DRX and partial dynamical recovery (DRV). The high density tangle dislocations in fine DRXed grains caused by extrusion deformation can be reduced via dislocation climb and elimination of opposite sign dislocations during the low speed extrusion [32]. Moreover, the low extrusion rate offers sufficient time to segregate Ag and Gd atoms at the site of dislocations (Fig. 2d). The Ag segregation phenomenon has been observed in cold-rolled Mg–Ag alloy in previous literature [33]. It has also been reported that the interaction of Ag atoms with dislocation occurs readily at 53 °C in Mg–10%Ag alloy [34]. The Ag atoms have a higher diffusivity in Mg compared with RE atoms [35,36] and a smaller radius of atom (1.44 Å) compared with that of Gd (1.80 Å) and Mg (1.60 Å), which are more capable of interacting with the dislocation for reducing the strain energy in Mg, and to form the Ag-pinning-dislocation condition in the DRXed grains. When the extrusion sample is aged during at 200 °C, the Ag and Gd atoms continue to segregate into dislocations for decrease the strain energy caused by the solute Ag and Gd atoms, and then the fine particles at dislocation are formed from the cluster of solute atom segregation (Fig. 5b). Therefore, we consider that the mobile dislocations pinned by solute atom segregation or fine particles are formed in the fine DRXed grains of extruded sample and peak-aged sample.

4.2. Yielding mechanism in the fine-grained age-type Mg alloy

In the fine-grained microstructure of Mg alloys, the non-basal dislocation slip but not twinning is always activated to satisfy the von-mises condition during deformation, and the activity of non-basal slip system is attributed to grain-boundary compatibility stress [6]. It has been reported that the yielding phenomenon appears in the tensile curves of the fine-grained AZ31 and Mg-3Gd alloys without secondary phase particles, which is related to the dislocation slip mechanism rather than twinning [6,7].

In this study, we find that the tensile stress-strain curves of fine-grained Mg-14Gd-2Ag-0.5Zr alloy containing a high volume fraction of particles show an obvious yielding phenomenon. It is considered that this yielding phenomenon is related to the existence of mobile dislocations pinned possibly by solute atom segregation or particles in the fine DRXed grains of extruded sample and peak-aged sample [37]. The mobile pinned-dislocations (MPDs), especially basal and prismatic <a> dislocations, can be activated near the grain boundary or the phase boundary at the initial stage of deformation when the extruded or peak-aged samples are tensile tested. To start these existing MPDs, the stress must be increased to overcome the dislocation pinning from the solute atom segregation or particles, and then the upper yielding point in the tensile curve is produced. However, when the pinning is unlocked, the dislocations can move along the slip plane under a comparatively low stress, and thus the lower yielding point occurs. Only some part of these MPDs need to be activated to satisfy the plastic deformation when the tensile test is conducted under a low strain rate of 10^{-3}/s, which can produce the wavy serration in the yielding plateau observed in the tensile curve. After all these MPDs are successively activated to contribute to plastic deformation, the yielding stage is completed accompanied with the end of the yielding plateau. It is found that the yielding plateau contributes ~6% strain in the peak-aged sample, while it contributes only ~2% strain in the extruded sample. On this phenomenon, we have the following explanation. In addition to the MPDs, some the dislocation-rearranged structures also exist in the extruded sample, which are difficult to be activated before the end of the yielding plateau during tensile test. The dissociation of the

dislocation-rearranged structure maybe occurs and the additional MPDs can be transformed from the partial dislocation-rearranged structure during aging. Therefore, the peak-aged sample has more MPDs. Furthermore, compared to the extruded sample, the higher yield stress in peak-aged sample during tensile test, which is caused by the precipitation in the interior of grains, can more effectively activate MPDs. Therefore, the yielding plateau of the peak-aged sample with more MPDs contributes to the larger strain. In addition, after the yielding stage, the work hardening rate of the extruded sample is higher than that of the peak-aged sample, and it is consistent with the inference that the more rearranged dislocations, difficult to be activated before the end of the yielding plateau during tensile test, exist in the extruded sample.

5. Conclusion

In this work, a new phenomenon of tensile yielding point in the fine-grained age-type Mg-14Gd-2Ag-0.5Zr alloy is found and discussed. The main conclusions are as follows:

(1) The fine-grained microstructure containing the mobile dislocations and dislocation-rearranged structure can be formed when the alloy is extruded at a relatively low temperature and low extrusion rate.
(2) A tensile yielding plateau phenomenon is observed in tensile curve at RT, which is attributed to the existence of mobile dislocations pinned possibly by the segregated solute atoms or particles within fine DRXed grains.
(3) The yielding plateau contributes ~6% strain in the peak-aged sample, while it contributes only ~2% strain in the extruded sample, suggesting that more MPDs are activated in the peak-aged sample during tensile test.

Originality statement

A new phenomenon of tensile yielding plateau in the fine-grained age-type Mg-14Gd-2Ag-0.5Zr alloy is reported. The yielding phenomenon is closely related to the activation of mobile pinned-dislocations (MPDs) formed by the segregation of solute atoms or particles at the site of mobile dislocations within the fine dynamic recrystallized (DRXed) grains during extrusion and aging treatment. The yielding plateau contributes ~6% strain in the peak-aged sample, while it contributes only ~2% strain in the extruded sample, suggesting the formation of more additional MPDs transformed from the partial dislocation-rearranged structure during aging. The formation of fine-grained microstructure and the yielding mechanism are discussed in detail. The results are helpful to design and control the microstructure of the age-type Mg alloys, and contribute to understand the deformation as well as strengthening mechanism of Mg alloys with fine-grained microstructure.

Declaration of competing interest

We declare that we have no financial and personal relationships with other people or organizations that can inappropriately influence our work, there is no professional or other personal interest of any nature or kind in any product, service and/or company that could be construed as influencing the position presented in, or the review of, the manuscript entitled, “Room temperature yielding phenomenon in extruded or/and aged Mg-14Gd-2Ag-0.5Zr alloy with fine-grained microstructure”. This paper has been neither copyrighted, classified, published, nor is being considered for publication elsewhere. If accepted, the article will not be published elsewhere in the same form, in any language, without the written consent of the publisher.

CRediT authorship contribution statement

R.G. Li: Writing - original draft, Conceptualization, Investigation, Methodology, Data curation, Supervision, Writing - review & editing. **D. Y. Zhao:** Investigation, Methodology, Data curation. **J.H. Zhang:** Writing - original draft, Investigation, Methodology, Writing - review & editing. **H.R. Li:** Investigation, Methodology, Data curation, Formal analysis. **Y.Q. Dai:** Investigation, Methodology. **D.Q. Fang:** Investigation, Writing - review & editing.

Acknowledgments

This work was supported by the National Natural Science Foundation of China (Grant Nos. 51971151 and 51871069), the project of Liaoning Province’s “rejuvenating Liaoning talents plan” (XLYC1907083), Natural Science Foundation of Liaoning Province of China (20180550299), Science Research Project of Liaoning Province Education Department (LQ2019002).

References

[1] T. Lee, C.H. Park, D. Lee, C.S. Lee, Enhancing tensile properties of ultrafine-grained medium-carbon steel utilizing fine carbides, Mater. Sci. Eng. A 528 (2011) 6558–6564.
[2] W. Wen, J.G. Morris, The effect of cold rolling and annealing on the serrated yielding phenomenon of AA5182 aluminum alloy, Mater. Sci. Eng. A 373 (2004) 204–216.
[3] O. Nijs, B. Holmedal, J. Friis, E. Nes, Sub-structure strengthening and work hardening of an ultra-fine grained aluminium-magnesium alloy, Mater. Sci. Eng. A 483–484 (2008) 51–53.
[4] B. Klusemann, G. Fischer, T. Böhlke, B. Svendsen, Thermomechanical characterization of Portevin-Le Châtelier bands in AlMg3 (AA5754) and modeling based on a modified Estrin–McCormick approach, Int. J. Plast. 67 (2015) 192–216.
[5] D. Zhang, H. Wen, M. Arul Kumar, F. Chen, L. Zhang, I.J. Beyerlein, J. M. Schoenung, S. Mahajan, E.J. Lavernia, Yield symmetry and reduced strength differential in Mg-2.5Y alloy, Acta Mater. 120 (2016) 75–85.
[6] J. Koike, T. Kobayashi, T. Mukai, H. Watanabe, M. Suzuki, K. Maruyama, K. Higashi, The activity of non-basal slip systems and dynamic recovery at room temperature in fine-grained AZ31B magnesium alloys, Acta Mater. 51 (2003) 2055–2065.
[7] X. Luo, Z.Q. Feng, T.B. Yu, J.Q. Luo, T.L. Huang, G.L. Wu, N. Hansen, X.X. Huang, Transitions in mechanical behavior and in deformation mechanisms enhance the strength and ductility of Mg-3Gd, Acta Mater. 183 (2020) 398–407.
[8] Y.N. Wang, J.C. Huang, The role of twinning and untwinning in yielding behavior in hot-extruded Mg–Al–Zn alloy, Acta Mater. 55 (2007) 897–905.
[9] O. Muránskya, M.R. Barnett, V. Luzinc, S. Vogel, On the correlation between deformation twinning and Lüders-like deformation in an extruded Mg alloy: in situ neutron diffraction and EPSC.4 modelling, Mater. Sci. Eng. A 527 (2010) 1383–1394.
[10] J. Wang, M.R.G. Ferdowsi, S.R. Kada, C.R. Hutchinson, M.R. Barnett, Influence of precipitation on yield elongation in Mg-Zn alloys, Scripta Mater. 160 (2019) 5–8.
[11] J.H. Zhang, S.J. Liu, R.Z. Wu, L.G. Hou, M.L. Zhang, Recent developments in high-strength Mg-RE-based alloys: focusing on Mg-Gd and Mg-Y systems, J. Magnes. Alloys 6 (2018) 277–291.
[12] T. Homma, N. Kunito, S. Kamado, Fabrication of extraordinary high-strength magnesium alloy by hot extrusion, Scripta Mater. 61 (2009) 644–647.
[13] J.P. Sun, B.Q. Xu, Z.Q. Yang, H. Zhou, J. Han, Y. Wu, D. Song, Y.C. Yuan, X. R. Zhuo, H. Liu, A.B. Ma, Achieving excellent ductility in high-strength Mg-10.6Gd-2Ag alloy via equal channel angular pressing, J. Alloys Compd. 817 (2020) 152688.
[14] X.C. Sha, L.R. Xiao, X.F. Chen, G.M. Cheng, Y.D. Yu, D.D. Yin, H. Zhou, Atomic structure of γ″ phase in Mg-Gd-Y-Ag alloy induced by Ag addition, Philos. Mag. 16 (2019) 1957–1969.
[15] L.R. Xiao, Y. Cao, S. Li, H. Zhou, X.L. Ma, L. Mao, X.C. Sha, Q.D. Wang, Y.T. Zhu, X. D. Han, The formation mechanism of a novel interfacial phase with high thermal stability in a Mg-Gd-Y-Ag-Zr alloy, Acta Mater. 162 (2019) 214–225.
[16] H. Zhou, G.M. Cheng, X.L. Ma, W.Z. Xu, S.N. Mathaudhu, Q.D. Wang, Y.T. Zhu, Effect of Ag on interfacial segregation in Mg–Gd–Y–(Ag)–Zr alloy, Acta Mater. 95 (2015) 20–29.
[17] Y. Zhang, Y.M. Zhu, W. Rong, Y.J. Wu, L.M. Peng, J.F. Nie, N. Birbilis, On the precipitation in an Ag-containing Mg-Gd-Zr alloy, Metall. Mater. Trans. A 49 (2018) 673–693.
[18] W.W. Jian, G.M. Cheng, W.Z. Xu, H. Yuan, M.H. Tsai, Q.D. Wang, C.C. Koch, Y. T. Zhu, N. Mathaudhu, Ultrastrong Mg alloy via nano-spaced stacking faults, Mater. Res. Lett. 1 (2013) 61–66.
[19] Q.D. Wang, J. Chen, Z. Zhao, S.M. He, Microstructure and super high strength of cast Mg-8.5Gd-2.3Y-1.8Ag-0.4Zr alloy, Mater. Sci. Eng. A 528 (2010) 323–328.
[20] A. Movahedi-Rad, R. Mahmudi, Effect of Ag addition on the elevated-temperature mechanical properties of an extruded high strength Mg-Gd-Y-Zr alloy, Mater. Sci. Eng. A 614 (2014) 62–66.

[21] S. Sandlöbes, S. Zaefferer, I. Schestakow, S. Yi, R. Gonzalez-Martinez, On the role of non-basal deformation mechanisms for the ductility of Mg and Mg-Y alloys, Acta Mater. 59 (2011) 429–439.
[22] K. Kim, J.B. Jeon, N.J. Kim, B. Lee, Role of yttrium in activation of <c+a> slip in magnesium: an atomistic approach, Scripta Mater. 108 (2015) 104–108.
[23] Z.G. Ding, W. Liu, H. Sun, S. Li, D.L. Zhang, Y.H. Zhao, E.J. Lavernia, Y.T. Zhu, Origins and dissociation of pyramidal <c+a> dislocations in magnesium and its alloys, Acta Mater. 146 (2018) 265–272.
[24] R.K. Sabat, A.P. Brahme, R.K. Mishra, K. Inal, S. Suwas, Ductility enhancement in Mg-0.2%Ce alloys, Acta Mater. 161 (2018) 246–257.
[25] S. Sandlöbes, M. Friák, J. Neugebauer, D. Raabe, Basal and non-basal dislocation slip in Mg–Y, Mater. Sci. Eng. A 576 (2013) 61–68.
[26] B.J. Wang, D.K. Xu, S.D. Wang, L.Y. Sheng, R.C. Zeng, E.H. Han, Influence of solution treatment on the corrosion fatigue behavior of an as-forged Mg-Zn-Y-Zr alloy, Int. J. Fatig. 120 (2019) 46–55.
[27] R.G. Li, H.B. Shafqat, J.H. Zhang, R.Z. Wu, G.Y. Fu, L. Zong, Y. Su, Cold-working mediated converse age hardening responses in extruded Mg-14Gd-2Ag-0.5Zr alloy with different microstructure, Mater. Sci. Eng. A 748 (2019) 95–99.
[28] J.P. Hadorn, T.T. Sasaki, T. Nakata, T. Ohkubo, S. Kamadob, K. Hono, Solute clustering and grain boundary segregation in extruded dilute Mg-Gd alloys, Scripta Mater. 93 (2014) 28–31.
[29] W.T. Sun, X.G. Qiao, M.Y. Zheng, C. Xu, S. Kamado, X.J. Zhao, H.W. Chen, N. Gao, Altered ageing behaviour of a nanostructured Mg-8.2Gd-3.8Y-1.0Zn-0.4Zr alloy processed by high pressure torsion, Acta Mater. 151 (2018) 260–270.
[30] W.T. Sun, X.G. Qiao, M.Y. Zheng, X.J. Zhao, H.W. Chen, N. Gao, M.J. Starink, Achieving ultra-high hardness of nanostructured Mg-8.2Gd-3.2Y-1.0Zn-0.4Zr alloy produced by a combination of high pressure torsion and ageing treatment, Scripta Mater. 155 (2018) 21–25.
[31] N. Mo, M. Carroll, Q.Y. Tan, A. Ceguerra, Y. Liu, J. Cairney, H. Dieringa, Y. D. Huang, B. Jiang, F.S. Pan, M. Bermingham, M.X. Zhang, Understanding solid solution strengthening at elevated temperatures in a creep-resistant Mg-Gd-Ca alloy, Acta Mater. 181 (2019) 185–199.
[32] K. Huang, R.E. Logé, A review of dynamic recrystallization phenomena in metallic materials, Mater. Des. 111 (2016) 548–574.
[33] L.R. Xiao, X.F. Chen, Y. Cao, H. Zhou, X.L. Ma, D.D. Yin, B. Ye, X.D. Han, Y.T. Zhu, Solute segregation assisted nanocrystallization of a cold-rolled Mg-Ag alloy during annealing, Scripta Mater. 177 (2020) 69–73.
[34] M. Chaturvedi, D.J. Lloyd, K. Tangri, Serrated yielding in magnesium–10 wt. % silver alloy, Met. Sci. J. 6 (1974) 16–19.
[35] M.C. Chaturvedi, D.J. Lloyd, Onset of serrated yielding in Mg-10Ag alloy, Philos. Mag. 30 (1974) 1199–1207.
[36] S.M. Zhu, J.F. Nie, Serrated flow and tensile properties of a Mg-Y-Nd alloy, Scripta Mater. 50 (2004) 51–55.
[37] B.J. Brindley, P.J. Worthington, Yield-point phenomena in substitutional alloys, Metall. Rev. 15 (1970) 101–114.